Investigation of the Atmospheric Oxidation Pathways of Bromoform and Dibromomethane: Initiation via UV Photolysis and Hydrogen Abstraction

W. Sean McGivern,[†,§] Hahkjoon Kim,[†] Joseph S. Francisco,[‡] and Simon W. North*[,†]

Department of Chemistry, Texas A&M University, 3255 TAMU, College Station, Texas 77842, and Department of Chemistry and Department of Earth and Atmospheric Sciences, Purdue University, West Lafayette, Indiana 47907-1393

Received: October 13, 2003; In Final Form: May 17, 2004

A computational study of the oxidation of CH_2Br_2 and $CHBr_3$ initiated via both UV photolysis and abstraction of an H atom by OH/Cl radicals has been performed. We have calculated the energetics associated with the addition of O_2 to the substituted bromomethyl radicals and the subsequent addition of NO to the peroxy radicals to form energized peroxy nitrite molecules. The peroxy nitrite molecules are predicted to dissociate rapidly to form alkoxy radicals (CH_2BrO and $CHBr_2O$) and NO_2, and the kinetics of these reactions have been determined using Rice−Ramsperger−Kassel−Marcus/master equation calculations. We additionally find that the reaction of the peroxy radicals with HO_2 may directly lead to significant production of alkoxy radicals, a pathway that is unimportant in nonbrominated analogues. We predict that the alkoxy radicals will dissociate rapidly via C−Br bond cleavage. The atmospheric implications of these results will be discussed.

Introduction

In the present study, we consider the tropospheric oxidation pathways of methyl bromide (CH_3Br), dibromomethane (CH_2Br_2), and bromoform ($CHBr_3$). The oxidation of each species closely resembles the standard tropospheric oxidation mechanism for saturated hydrocarbons. Initiation of the oxidation proceeds via either abstraction of hydrogen atom by OH/Cl or via photolytic cleavage of a carbon−bromine bond

$$RH + OH/Cl \rightarrow R + H_2O/HCl \quad (1a)$$

$$RBr \xrightarrow{h\nu} R + Br \quad (1b)$$

The OH/Cl-initiated oxidation of bromoform was the subject of a previous computational study by some of the authors,[1] and the present study represents an extension of the earlier work to encompass the remainder of the brominated methane series. We focus on the fate of the radicals formed in parts a and b of eq 1 under atmospheric conditions. As shown in Figure 1, a computational study of the oxidation of CBr_3, $CHBr_2$, and CH_2Br provides information on all of the important oxidation pathways for the entire brominated methane series with the exception of reactions initiated by photolysis of CH_3Br to form methyl radicals and free Br atoms. The oxidation of methyl radicals is well understood in both the atmospheric and combustion chemistry literature,[2] and its study was omitted from the present work.

The oxidation mechanisms of the radical species shown in Figure 1 are similar. In the troposphere, the substituted methyl radicals initially react with ambient O_2 to form haloalkyl peroxy radicals

$$CH_2Br + O_2 \rightarrow CH_2BrO_2$$
$$CHBr_2 + O_2 \rightarrow CHBr_2O_2$$
$$CBr_3 + O_2 \rightarrow CBr_3O_2 \quad (2)$$

In the presence of NO, the haloalkyl peroxy radicals form energized peroxy nitrite molecules, which may either undergo collisional stabilization to form stable peroxy nitrite molecules or dissociation to form haloalkoxy radicals and NO_2

$$CH_2BrO_2 + NO \rightarrow CH_2BrOONO^* \begin{array}{l} \rightarrow CH_2BrO^* + NO_2 \\ \xrightarrow{M} CH_2BrOONO \end{array}$$
$$CHBr_2O_2 + NO \rightarrow CHBr_2OONO^* \begin{array}{l} \rightarrow CHBr_2O^* + NO_2 \\ \xrightarrow{M} CHBr_2OONO \end{array}$$
$$CBr_3O_2 + NO \rightarrow CBr_3OONO^* \begin{array}{l} \rightarrow CBr_3O^* + NO_2 \\ \xrightarrow{M} CBr_3OONO \end{array} \quad (3)$$

Although the energized nitrite molecules can isomerize to the more favorable nitrate isomers, there is no experimental or theoretical evidence for this channel. The resulting haloalkoxy radicals are highly activated and, as discussed below, can undergo decomposition along the C−Br bond to form an aldehydic species and free Br atoms

$$CH_2BrO^* \rightarrow CH_2O + Br$$
$$CHBr_2O^* \rightarrow CHBrO + Br$$
$$CBr_3O^* \rightarrow CBr_2O + Br \quad (4)$$

On the basis of the analogous reactions of fluoromethoxy and chloromethoxy radicals, the CH_2BrO and $CHBr_2O$ radicals

* To whom correspondence may be addressed. E-mail: swnorth@tamu.edu.
† Texas A&M University.
‡ Purdue University.
§ Present address: Physical and Chemical Properties Division, National Institute of Standards and Technology, 100 Bureau Drive, Gaithersburg, MD 20876-8381.

10.1021/jp0311613 CCC: $27.50
Published on Web 08/05/2004

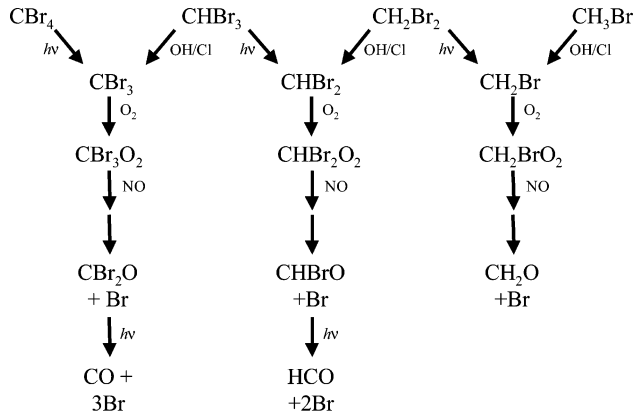

Figure 1. Schematic diagram of initiation pathways in the tropospheric oxidation of the brominated methane series.

might also be expected to react with oxygen

$$CH_2BrO + O_2 \rightarrow CHBrO + HO_2$$

$$CHBr_2O + O_2 \rightarrow CBr_2O + HO_2 \quad (5)$$

in competition with decomposition. In addition, other reactions of the haloalkyl peroxy radicals may be important in low NO_x environments, including reaction with HO_2.

In the present work, we have determined the energetics for the processes shown in eqs 2−4 using ab initio techniques. We have subsequently performed Rice−Ramsperger−Kassel−Marcus/master equation (RRKM/ME)[3,4] calculations using the calculated geometries, frequencies, and energies to assess the relative importance of each of these pathways under ambient conditions in the upper and lower troposphere. On the basis of these results, the atmospheric implications of the dominant mechanistic pathways are discussed.

Calculations

The energetics were calculated using the coupled cluster with single and double excitations and perturbative treatment of the triple excitations method (CCSD(T)) with the triple-ζ correlation-consistent polarized valence basis set of Dunning and coworkers (cc-pVTZ).[5−7] The geometries and frequencies were evaluated at the second-order Moller−Plesset (MP2) level using the 6-311+G* Pople-style basis set. Full treatment of the core electrons was used in the calculation of geometries and frequencies (MP2(FULL)), and only the valence electrons were correlated (frozen core approximation) in the coupled-cluster energy calculations. On the basis of previous work with halocarbon species, these levels of theory were found to represent a good compromise between the treatment of electron correlation, basis-set size, and computational expense.[8] All reported relative energies are zero-point corrected using unscaled frequencies. All calculations were performed using Gaussian 98.[9] We find that there is little difference between the MP2/6-311+g(d,p) and MP2/aug-cc-pVDZ energetics. For example, the difference in results is 1.2 kcal/mol for the CH_2BrO case and 0.2 kcal/mol for the $CHBr_2O$ case. We find that the two basis sets provide comparable results.

To check whether the transition states for the dissociation of CH_2BrO and $CHBr_2O$ connected to the dissociation products CH_2O + Br and CHBrO + Br, respectively, intrinsic reaction coordinate (IRC) calculations[10] were performed at the UMP2/6-31G(d) level of theory. Calculations run in the forward direction showed the C−Br bond breaking and the UMP2/6-31G(d) energies converging toward the energies of the separated product energies. IRC calculations were also run in the reverse direction to confirm that the transition states connected to the stable CH_2BrO and $CHBr_2O$ radicals.

TABLE 1: Total Energies (Hartrees) and Zero-Point Energies for Species Involved in the Oxidation of $CHBr_2$[a]

species	CCSD(T)/cc-pVTZ	ZPE
$CHBr_2O$ ($^2A'$)	−5259.088060	0.019 380
$CHBr_2O^‡$ ($^2A'$)	−5259.091063	0.018 574
CHBrO	−2686.458055	0.018 697
$CHBr_2$ ($^2A'$)	−5183.969055	0.015 511
$CHBr_2O_2$	−5334.146564	0.024 361
$CHBr_2OOH$	−5334.799958	0.036 149
$CHBr_2OONO$	−5463.905387	0.031 391
O (^3P)	−74.973962	N/A
Br (^2P)	−2572.661119	N/A
HO_2 ($^2A''$)	−150.712007	0.014 613
O_2 ($^3\Sigma$)	−150.128898	0.003 328
OH ($^2\Pi$)	−75.637567	0.008 607
NO ($^2\Pi$)	−129.716038	0.008 036
NO_2	−204.800012	0.010 733

[a] Geometries and zero-point corrections were obtained at the MP2/6-311+G* level.

To check the reliability of the CCSD(T)/cc-pVTZ//MP2/6-311+g* method for bromine reactions, we have compared calculated results with well-known experimental heats of formation[11] and higher-level theory.[12] These reactions are

$$CHBrO \rightarrow HCO + Br \quad (6)$$

$$CHBr \rightarrow CH + Br \quad (7)$$

$$CBr_2 \rightarrow CBr + Br \quad (8)$$

We find that the heat of reactions for each is 67.3, 78.0, and 63.0 kcal/mol for reactions 6−8, respectively, using the CCSD(T)/cc-pVTZ//MP2/6-311+G* method that we have employed in the present manuscript. This compares favorably with values of 68.0, 77.8, and 61.2 kcal/mol, respectively, based on the experimental heat of formations. The root-mean-square error is 1.4 kcal/mol between CCSD(T)/cc-pVTZ//MP2/6-311+G* and experiment. A conservative estimate of the error associated with the energetics in our study is likely to be ±3 kcal/mol with our method. In addition, most of the reactions in the present study involve loose transition states, and consequently, modest errors in the binding energies will not alter the conclusions. Our finding that the transition states associated with Br elimination from the alkoxy radicals are minimal (vide supra) suggests that small errors (±2 kcal/mol) in these barriers will still not change the chemistry.

Results and Discussion

Total energies for the species relevant to the oxidation of CH_2Br and $CHBr_2$ are shown in Tables 1 and 2 at the CCSD(T)/cc-pVTZ//MP2(FULL)/6-311+G* level. The relative energetics for the mechanistic steps shown in eqs 2−4 are shown in Figure 2 for the oxidation of CH_2Br and in Figure 3 for the oxidation of $CHBr_2$. In both cases, the addition of O_2 to the halomethyl radical was found to be strongly exothermic. The degree of exothermicity was observed to decrease with increasing bromine substitution of the reactant bromomethyl radical, ranging from 29.8 kcal/mol for CH_2Br to 16.7 kcal/mol for CBr_3 (ref 1). A transition state for the addition of O_2 to CBr_3 was observed previously at the CCSD(T)/cc-pVTZ level.[1] However, based on the large reaction rates associated with this addition reaction and the observation that basis-set effects continued to be important even at the CCSD(T)/cc-pVTZ level, it was assumed

TABLE 2: Total Energies (Hartrees) and Zero-Point Energies for Species Involved in the Oxidation of CH_2Br[a]

species	CCSD(T)/cc-pVTZ	ZPE
CH_2BrO ($^2A'$)	−2686.981791	0.029007
$CH_2BrO^‡$ ($^2A'$)	−2686.980831	0.028479
CH_2BrO ($^2A''$)	−2686.976953	0.029007
$CH_2BrO^‡$ ($^2A''$)	−2686.950503	0.028479
CH_2Br ($^2A'$)	−2611.870655	0.022852
CH_2BrO_2 ($^2A''$)	−2762.047019	0.034517
CH_2BrOOH	−2762.693046	0.046311
$CH_2BrOONO$	−2891.801429	0.041703

[a] Geometries and zero-point corrections were obtained at the MP2/6-311+G* level.

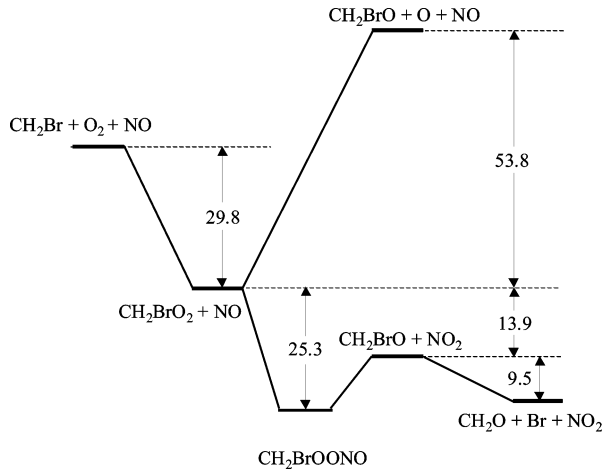

Figure 2. Schematic relative energy diagram for the oxidation of CH_2Br in the presence of O_2 and NO to form CH_2O and free Br atoms. All energies (CCSD(T)/cc-pVTZ) are zero-point corrected and are given in kcal/mol.

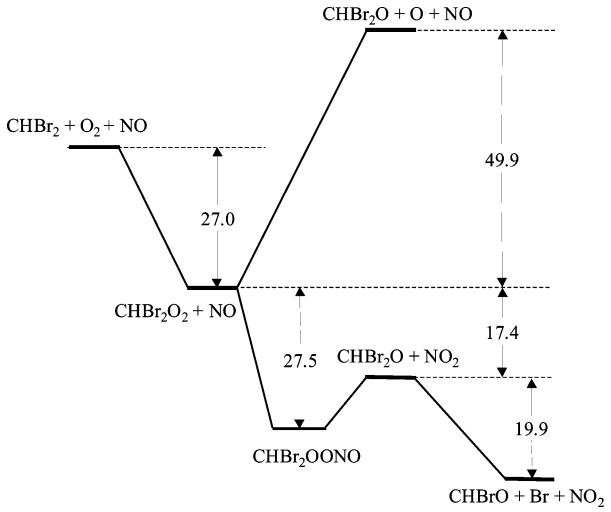

Figure 3. Schematic relative energy diagram for the oxidation of $CHBr_2$ in the presence of O_2 and NO to form CHBrO and free Br atoms. All energies (CCSD(T)/cc-pVTZ) are zero-point corrected and are given in kcal/mol.

that the reaction occurred along a barrierless potential. As a consequence, we assume that the O_2 addition reactions to CH_2Br and $CHBr_2$ also proceed along barrierless potentials and have not attempted to locate transition states for these reactions. Because of the large atmospheric number density of O_2 ($\sim 10^{18}$ molecules cm^{-3}), this reaction is expected to occur on an extremely fast time scale ($<10^{-6}$ s) relative to that of the initiation step and the subsequent reactions of the peroxy radicals with NO. In addition, the relatively low atmospheric concentrations of species with high reactivity toward the peroxy radicals (primarily NO and HO_2) will ensure that the RO_2 species are completely thermalized prior to further reaction. The reaction steps that follow the formation of the RO_2 species will therefore be discussed in turn in significantly greater detail.

The RO_2 + NO Reaction. Under typical atmospheric conditions, the thermalized brominated methyl peroxy radicals will react primarily with NO radicals. The reaction of RO_2 with NO proceeds via the addition of NO to form an activated peroxy nitrite molecule (ROONO*). The resulting ROONO* species may then either undergo collisional stabilization to form (ROONO) or dissociation to form an alkoxy radical (RO) and NO_2. The relative importance of these two pathways is determined by the stability of the ROONO species relative to the exothermicity of the abstraction reaction and the role of collisional energy transfer. The difference between the energies associated with these pathways is found to decrease with increasing bromine substitution. In CH_2BrO_2 (Figure 2), the difference between the CH_2BrO + NO_2 products and the $CH_2BrOONO$ molecule is found to be 11.4 kcal/mol. The difference decreases to 9.9 kcal/mol in the case of $CHBr_2O_2$ (Figure 3), while the difference was previously found to be only 3.3 kcal/mol in CBr_3O.[1] This trend implies a weakening of the O−O bond in the peroxy radicals upon increasing bromine substitution. This trend is not transparent from a comparison of the O−O bond lengths in each species that were found to be 1.296, 1.303, and 1.300 Å in CH_2BrO_2, $CHBr_2O_2$, and CBr_3O_2, respectively.

To evaluate the importance of these energetic differences, we have performed RRKM/ME calculations to obtain the relative importance of the stabilization and abstraction channels. The activated nitrite distribution was obtained from a variational RRKM treatment of the RO_2 + NO reaction.[13] The collisional transition probabilities were calculated using an exponential gap model with $\Delta E = 250$ cm^{-1}. The internal energy distributions of the nascent alkoxy radicals were obtained using the separate statistical ensembles method to describe the energy partitioning.[14,15] As was found previously for the CBr_3O_2 + NO reaction, the reactions of CH_2BrO_2 and $CHBr_2O_2$ with NO were found to exclusively form the alkoxy radical product with no apparent stabilization of the peroxy nitrite species for pressures ranging from 300 to 700 Torr at temperatures from 240 to 300 K, which span the typical range of pressures and temperatures in the troposphere. The formation of stable nitrate species, $RONO_2$, from isomerization of the activated peroxy nitrite molecule may, in principle, provide a means of removal of the peroxy radicals. An accurate theoretical description for the isomerization process remains challenging[16−18] and was not included in the present study.

The RO Reactions. The reactions of the alkoxy radicals derived from the RO_2 + NO reaction play an important role in determining the final end product yields. For small haloalkoxy radicals, the reactions of primary importance are decomposition and reaction with O_2. Typical values of the rate constant for H abstraction by O_2 (10^{-14} cm^3 s^{-1})[25] correspond to rates on the order of 10^4 s^{-1} under ambient conditions. We have evaluated the energetics associated with the decomposition of the bromoalkoxy radicals to form an aldehyde and free bromine atom. Both species are of C_s symmetry, leading to $^2A'$ and $^2A''$ components associated with the unpaired electron on the oxygen p_x or p_y orbital. The ground-state-optimized geometries of the two states were found to be similar in both CH_2BrO and $CHBr_2O$. In CH_2BrO, both states correlate to the same dissociation products, namely, atomic bromine and CH_2O. In CH_2BrO, the $^2A'$ state is found to be 3.0 kcal/mol lower in

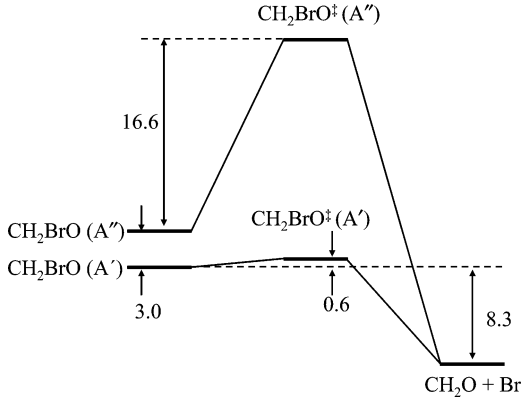

Figure 4. Schematic relative energy diagram for the dissociation of CH_2BrO on A′ and A″ surfaces. All energies (CCSD(T)/cc-pVTZ) are zero-point corrected and are given in kcal/mol.

energy than the $^2A''$ state at the CCSD(T)/cc-pVTZ level. The energetics associated with Br elimination from CH_2BrO from the $^2A'$ and the $^2A''$ states are shown in Figure 4. The transition state on the $^2A'$ surface is 0.6 kcal/mol above the reactant for CH_2BrO, while the $^2A''$ state transition state is 16.6 kcal/mol. Our previous study[1] on CBr_3O suggests that extrapolation to the infinite basis-set limit[8] would likely place the transition state below the reactant energy for the $^2A'$ state in CH_2BrO. The transition state for $CHBr_2O$ lies 2.4 kcal/mol below the reactant, also consistent with a barrierless reaction. In addition, RRKM/ME calculations of the $RO_2 + NO$ reaction predict alkoxy radical energy distributions that lie well above the reactant minimum. Since the RO species dissociates along a barrierless potential, the alkoxy radical is expected to undergo prompt dissociation prior to collisional stabilization.

Wu and Carr have performed G2 and G2(MP2) calculations of the energetics for the analogous reactions of CH_2ClO.[19] Geometries of the ground state as well as the transition states for Cl and HCl loss were identified at the MP2(FULL)/6-31G(d,p) level. As in the present work, two distinct ground-state structures with symmetries A′ and A″ were observed; however, those authors did not identify separate A″ transition states for the possible loss channels. Both loss channels were found to have well-defined transition-state structures and energies. The HCl loss channel was found to have a barrier of 8.0 kcal/mol at the G2(MP2) level, and the Cl loss channel was found to have a barrier of 10.5 kcal/mol. RRKM calculations were performed for each channel and were found to reproduce the experimental temperature dependence for critical energies within 1 kcal/mol of the ab initio results. The authors observed that the branching to the Cl loss channel was unimportant relative to the HCl channel for atmospherically relevant temperatures and pressures. However, based on previous experimental work by Wu and Carr,[20] the reactions of CH_2ClO analogous to those in eq 5 were found to dominate under all temperatures and pressures found in the troposphere.

The reactions of $CHCl_2O$ have been examined computationally by Hou et al.[21] The authors found that the Cl-loss reaction was exothermic by 10.5 kcal/mol with a barrier of 2.2 kcal/mol. The HCl-loss channel was found to be more strongly exothermic (22.9 kcal/mol) but had a 14.2 kcal/mol barrier to reaction. On the basis of these calculations, the HCl channel is predicted to be of significantly lesser importance than the Cl-loss channel, in contrast to the dissociation of CH_2ClO, where the HCl-loss channel was found to dominate. Li and Francisco have examined the C−F and C−Cl bond dissociation energies in the CF_3O and CCl_3O radicals.[22] In the case of CF_3O, the fluorine-loss reaction was found to be endothermic by 25.2 kcal/mol with a barrier of 29.1 kcal/mol. The cleavage of the C−Cl bond in CCl_3O, however, was predicted to be strongly exothermic ($\Delta E = -16.8$ kcal/mol) with a small forward barrier (1.3 kcal/mol). Hydrogen substitution of either species is not expected to significantly alter the C−X energetics.[23]

The fate of the CH_2BrO and $CHBr_2O$ radicals differs significantly from that of the analogous chlorine species. The absence of a significant barrier to dissociation will drive the reaction of the activated RO species exclusively toward the Br-loss channels. Since the HBr-loss channel will occur through a tighter transition state, it is not expected to be competitive with Br loss. In addition, the lifetimes of the activated CH_2BrO and $CHBr_2O$ radicals are expected to be so sufficiently short that the reaction with O_2 (reaction) will be negligible.

The oxidation of CH_2Br has been studied experimentally by Orlando et al.[24] Those authors used Fourier transform infrared absorption spectroscopy to probe the possible reaction products in chamber studies of methyl bromide oxidation under conditions of both high NO and NO-free environments. The reactions were initiated by UV photolysis of Cl_2, and the CH_2O, CO, and CHBrO concentrations were monitored. Those authors found that, in the presence of NO, Br loss from CH_2BrO was the dominant channel with no apparent evidence for the $CH_2BrO + O_2 \rightarrow CHBrO + HO_2$ or HBr-loss reactions found in the analogous chlorine systems. The present results, therefore, are consistent with the conclusions of the chamber experiments.

The $RO_2 + HO_2$ Reaction. Under conditions of moderate (>30 ppt) NO concentrations, the RO_2 radical is expected to react primarily with NO. However, in remote areas characterized by low NO concentrations, such as rural or marine regions, other reactions are important. The reaction of alkyl peroxy radicals and HO_2 provides a pathway for the formation of alkoxy radicals in the absence of NO or a means to form relatively stable hydroperoxide molecules

$$\begin{aligned} CH_2BrO_2 + HO_2 &\rightarrow CH_2BrO + OH + O_2 \\ &\rightarrow CH_2BrOOH + O_2 \\ CHBr_2O_2 + HO_2 &\rightarrow CHBr_2O + OH + O_2 \\ &\rightarrow CHBr_2OOH + O_2 \\ CBr_3O_2 + HO_2 &\rightarrow CBr_3O + OH + O_2 \\ &\rightarrow CBr_3OOH + O_2 \end{aligned} \quad (9)$$

We have calculated the energetics associated with each of these reaction pathways. The reaction of CBr_3O_2 with HO_2 was not considered in our previous work[1] and is presented here. Typically, the reactions of peroxy radicals with HO_2 exhibit an inverse temperature dependence,[25] implying that the system passes through a stable intermediate prior to dissociation. We have made no attempt to locate these intermediate ROOHOO structures. The energetics for each of the reactions in eq 9 are shown in Figure 5. The energy associated with the formation of alkoxy radicals relative to that of the reactants was found to decrease with increasing bromine substitution. The reaction of HO_2 with CH_2BrO was found to be endothermic by 1.2 kcal/mol, while the reactions of $CHBr_2O$ and CBr_3O are exothermic by 2.7 and 6.5 kcal/mol, respectively.

We have performed RRKM/ME calculations, based on several severe approximations, to qualitatively estimate the relative importance of the reactions in eq 9 in the atmosphere. We have assumed that the distribution of the ROOH species can be

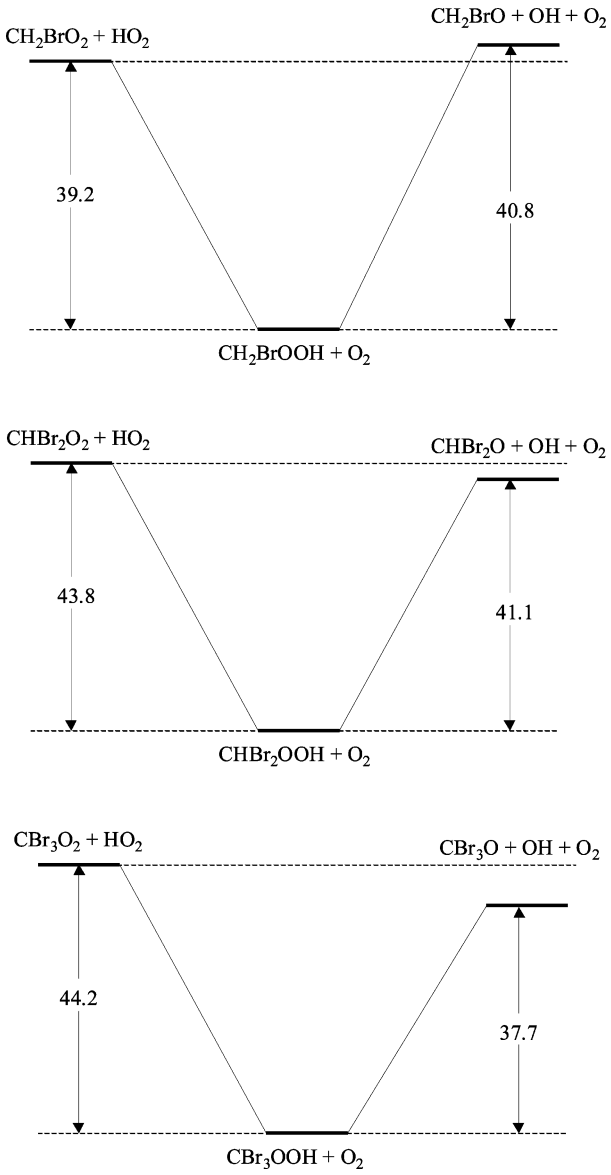

Figure 5. Schematic relative energy diagrams for the reactions of CH_2BrO, $CHBr_2O$, and CBr_3O with HO_2. All energies (CCSD(T)/cc-pVTZ) are zero-point corrected and are given in kcal/mol.

TABLE 3: Fractional Branching Ratios for the Formation of Prompt Alkoxy Radicals from the Reaction of Bromoalkyl Peroxy Radicals with HO_2

temperature/ pressure	CH_2BrO branching	$CHBr_2O$ branching	CBr_3O branching
300 K/ 760 Torr	0.062	0.36	0.66
240 K/ 350 Torr	0.039	0.41	0.73

approximated by a Boltzmann distribution with the zero of energy placed at the reactant ($RO_2 + HO_2$) energy. This is tantamount to assuming that the O_2 acts as a spectator and that the energy partitioning associated with the break-up of the ROOHOO species is statistical. In general, an RRKM or variational RRKM calculation using information on the ROOHOO intermediate combined with the separate statistical ensembles model partitioning of energy will provide a more accurate ROOH energy distribution. However, we believe that approximate treatment provides an insightful first-order assessment of the relative importance of these reactions. The results of these calculations are shown in Table 3. In the case of the endothermic $CH_2BrO_2 + HO_2 \rightarrow CH_2BrO + OH + O_2$ reaction, we find that the branching to form prompt alkoxy radicals is small. The exothermic reactions of $CHBr_2O_2$ and CBr_3O_2 produce significantly larger fractions of alkoxy radicals directly, in contrast to the analogous reactions of chlorinated and nonhalogenated alkyl peroxy radicals. These analogous systems produce only a minor fraction of alkoxy radicals, strongly favoring the formation of the peroxide species.

Chamber studies by Orlando et al. on the oxidation of CH_3Br in the absence of NO revealed no evidence for the formation of CH_2BrOOH. In those studies, the observed decrease in the CH_3Br concentration due to hydrogen abstraction by Cl and photolysis completely accounted for the observed appearance of CH_2O, CHBrO, and CO products to within experimental error. We find that the self-reaction $CH_2BrO_2 + CH_2BrO_2 \rightarrow CH_2BrO + CH_2BrO + O_2$ is exothermic by 3.9 kcal/mol, which provides an alternative pathway for the formation of CHBrO in the absence of NO or HO_2. In the chamber studies of Orlando et al., the concentration of CH_2BrO_2 radicals will be significantly higher than in a typical atmospheric environment and the concentration of HO_2 radicals will be significantly lower. Thus the self-reaction may be the dominant source of reaction in this system in the absence of NO, and the observed end products are not sensitive to the reaction with HO_2. The $CHBr_2O_2$ self-reaction was found to be significantly more exothermic (−11.6 kcal/mol) and would be expected to exclusively form $CHBr_2O$ radicals under conditions in which the reaction is important. As noted previously, the CBr_3O_2 self-reaction is exothermic by 20.0 kcal/mol[1] and is also expected to provide a pathway for the formation of alkoxy radicals that undergo subsequent decomposition.

Conclusions

The energetics of species relevant to the atmospheric oxidation of CH_2Br_2 and $CHBr_3$ have been examined using ab initio methods. The oxidation mechanisms of CH_2Br and $CHBr_2$ were found to be similar. The initial addition reactions of O_2 to form alkoxy peroxy radicals are strongly exothermic, and the subsequent reactions with NO in high NO_x atmospheric environments were calculated to produce alkoxy radicals, CH_2BrO and $CHBr_2O$, in yields near unity. Unlike in analogous chlorine- and fluorine-containing systems, facile cleavage of the C−Br bonds in the alkoxy radicals is predicted to occur for both species, due to the lack of an appreciable barrier to dissociation. In addition, under low NO_x conditions, the reaction of alkoxy peroxy radicals (RO_2) with HO_2 were found to yield significant fractions of both alkoxy radicals and stable peroxide molecules (ROOH) with a strong dependence on the local ambient temperatures and pressures.

Acknowledgment. The authors would like to thank Dr. Lisa Perez for useful comments regarding the ab initio calculations. Jiho Park is acknowledged for assistance with rate calculations. Hardware and software support from the Texas A&M University Supercomputing Facility and the Texas A&M University Laboratory for Molecular Simulations under the National Science Foundation Grant No. CHE-9528196 is acknowledged. WSM, H.K., and S.W.N. thank the Robert A. Welch Foundation (A-1405) for support.

Supporting Information Available: Optimized MP2/6-311+G* geometries and UHF $\langle s^2 \rangle$ expectation values prior to spin-annihilation for all molecules found in Tables 1 and 2. This material is available free of charge via the Internet at http://pubs.acs.org.

References and Notes

(1) McGivern, W. S.; Francisco, J. S.; North, S. W. *J. Phys. Chem. A* **2002**, *106*, 6395.

(2) Baldwin, A. L.; Golden, D. M. *Chem. Phys. Lett*. **1978**, *55*, 350. (b) Slagle, I. R.; Gutman, D. *J. Am. Chem. Soc*. **1985**, *107*, 5342. (c) Yu, C. L.; Wang, C.; Frenklach, M., *J. Phys. Chem*. **1995**, *99*, 14377. (d) Lary, D. J.; Toumi, R. *J. Geophys. Res*. A. **1997**, *102*, 23421.

(3) Holbrook, K. A.; Pilling, M. A.; Robertson, S. H. *Unimolecular Reactions*, 2nd ed.; Wiley-Interscience: New York, 1996.

(4) Baer, T.; Hase, W. L. *Unimolecular Reaction Dynamics*; Oxford: New York, 1996.

(5) Wilson, A. K.; Woon, D. E.; Peterson, K. A.; Dunning, T. H. *J. Chem. Phys* **1999**, *11*0, 7667.

(6) Dunning, T. H., Jr. *J. Chem. Phys.* **1989**, *90*, 1007.

(7) Woon, D. E.; Dunning, T. H., Jr. *J. Chem. Phys.* **1993**, *9*8, 1358.

(8) McGivern, W. S.; Derecskei-Kovacs, A.; North, S. W.; Francisco, J. S. *J. Phys. Chem. A* **2000**, *104*, 436.

(9) Frisch, M. J.; Trucks, G. W.; Schlegel, H. B.; Scuseria, G. E.; Robb, M. A.; Cheeseman, J. R.; Zakrzewski, V. G.; Montgomery, J. A., Jr.; Stratmann, R. E.; Burant, J. C.; Dapprich, S.; Millam, J. M.; Daniels, A. D.; Kudin, K. N.; Strain, M. C.; Farkas, O.; Tomasi, J.; Barone, V.; Cossi, M.; Cammi, R.; Mennucci, B.; Pomelli, C.; Adamo, C.; Clifford, S.; Ochterski, J.; Petersson, G. A.; Ayala, P. Y.; Cui, Q.; Morokuma, K.; Malick, D. K.; Rabuck, A. D.; Raghavachari, K.; Foresman, J. B.; Cioslowski, J.; Ortiz, J. V.; Stefanov, B. B.; Liu, G.; Liashenko, A.; Piskorz, P.; Komaromi, I.; Gomperts, R.; Martin, R. L.; Fox, D. J.; Keith, T.; Al-Laham, M. A.; Peng, C. Y.; Nanayakkara, A.; Gonzalez, C.; Challacombe, M.; Gill, P. M. W.; Johnson, B. G.; Chen, W.; Wong, M. W.; Andres, J. L.; Head-Gordon, M.; Replogle, E. S.; Pople, J. A. *Gaussian 98*, revision A.6; Gaussian, Inc.: Pittsburgh, PA, 1998.

(10) Gonzalez, C.; Schlegel, H. B. *J. Phys. Chem*. **1989**, *90*, 2154.

(11) Glukhovtsev, M. N.; Bach, R. D. *J. Phys. Chem*. A. **1997**, *101*, 3574.

(12) Dixon, D. A.; deJong, W. A.; Peterson, K. A.; Francisco, J. S. *J. Phys. Chem. A* **2002**, *106*, 4725.

(13) Park, J.; Stephens, J. S.; Zhang, R.; North, S. W. *J. Phys. Chem. A* **2003** submitted.

(14) Wittig, C.; Nadler, I.; Reisler, H.; Noble, M.; Catanzarite, J.; Radhakrishnan, G. *J. Chem. Phys.* **1985**, *83*, 5581.

(15) Vereecken, L.; Peeters, J.; Orlando, J. J.; Tyndall, G. S.; Ferronato, C. *J. Phys. Chem. A* **1999**, *103*, 4693−4702.

(16) Ellison, G. B.; Blanksby, S. J.; Jochnowitz, E. B.; Stanton, J. F. *Science*, submitted.

(17) Lohr, L. L.; Barker, J. R.; Shroll, R. *J. Chem. Phys.*, submitted.

(18) Zhang, D.; Zhang, R.; Park, J.; North S. W. *J. Am. Chem. Soc.* **2002**, *124*, 9600.

(19) Wu, F.; Carr, R. W. *J. Phys. Chem. A* **2002**, *106*, 5832.

(20) Wu, F.; Carr, R. W. *Chem. Phys. Lett.* **1999**, *305*, 44.

(21) Hou, H.; Wang, B.; Gu, Y. *J. Phys. Chem. A* **1999**, *103*, 8075.

(22) Li, Z.; Francisco, J. S. *J. Am. Chem. Soc*. **1989**, *111*, 5660.

(23) Dibble, T. S. *J. Mol Struct.* **1999**, *485*−*486*, 67.

(24) Orlando, J. J.; Tyndall, G. S.; Wallington, T. J. *J. Phys. Chem.* **1996**, *100*, 7026.

(25) DeMore, W. B.; Sander, S. P.; Howard, C. J.; Ravishankara, A. R.; Golden, D. M.; Kolb, C. E.; Hampson, R. F.; Kurylo, M. J.; Molina, M. J. Chemical Kinetics and Photochemical Data for Use in Stratospheric Modeling. *JPL Publication 97-4*; Jet Propulsion Lab: Pasadena, CA, 1997.